V. OPTICAL AND INFRARED SPECTROSCOPY*

Academic and Research Staff

Prof. C. H. Perry
Dr. R. P. Lowndes

Graduate Students

J. F. Parrish
N. E. Tornberg

A. REFLECTION MEASUREMENTS ON SOME ALKALI HALIDES IN THE FAR INFRARED

1. Introduction

The alkali halide materials investigated included KCl, KBr, KI, and RbI, all of which have the NaCl structure. The transmission of thin films of these materials as a function of temperature have been reported by others.[1,2] The object of this work was to perform reflectance measurements on single-crystal samples at various temperatures (300, 195, 80 and ~10°K) and to group these results with those obtained by using other techniques. The data were analyzed by a Kramers-Kronig method and were also fitted with a classical oscillator model. In nearly all cases the presence of two additional oscillators had to be included and these were ascribed to combinations of different phonon branches at critical points at the edge of the Brillouin zone.

2. Experiment

The interferometer and low-temperature detector used in these measurements have been described previously.[3] The reflectance values as shown in Figs. V-1 and V-2 are relative to the reflectivity of a front-aluminized mirror and the measurements were made at an angle of incidence of 10°. The low-temperature measurements were obtained by using an evacuated cryostat with polyethylene windows. The temperature was measured with calibrated copper-constantan thermocouples and a GE resistance thermometer attached to the samples.

The measured reflectivity spectral profiles for KCl, KBr, KI, RbI at 300, 195, 80 and 10°K are shown in Figs. V-1 and V-2. The main reststrahlen peak has usually one or two side bands on the high-frequency side. The reflectivity values are accurate to ±3% at the peak. This accuracy was established by taking an average of five or six measurements at each temperature.

*This work was supported in part by the Joint Services Electronics Programs (U. S. Army, U.S. Navy, and U. S. Air Force) under Contract DA 28-043-AMC-02536(E), and in part by the U. S. Air Force Cambridge Research Laboratories Contract AF 19(628)-6066, and the National Aeronautics and Space Administration (Grant NGR-22-009-237).

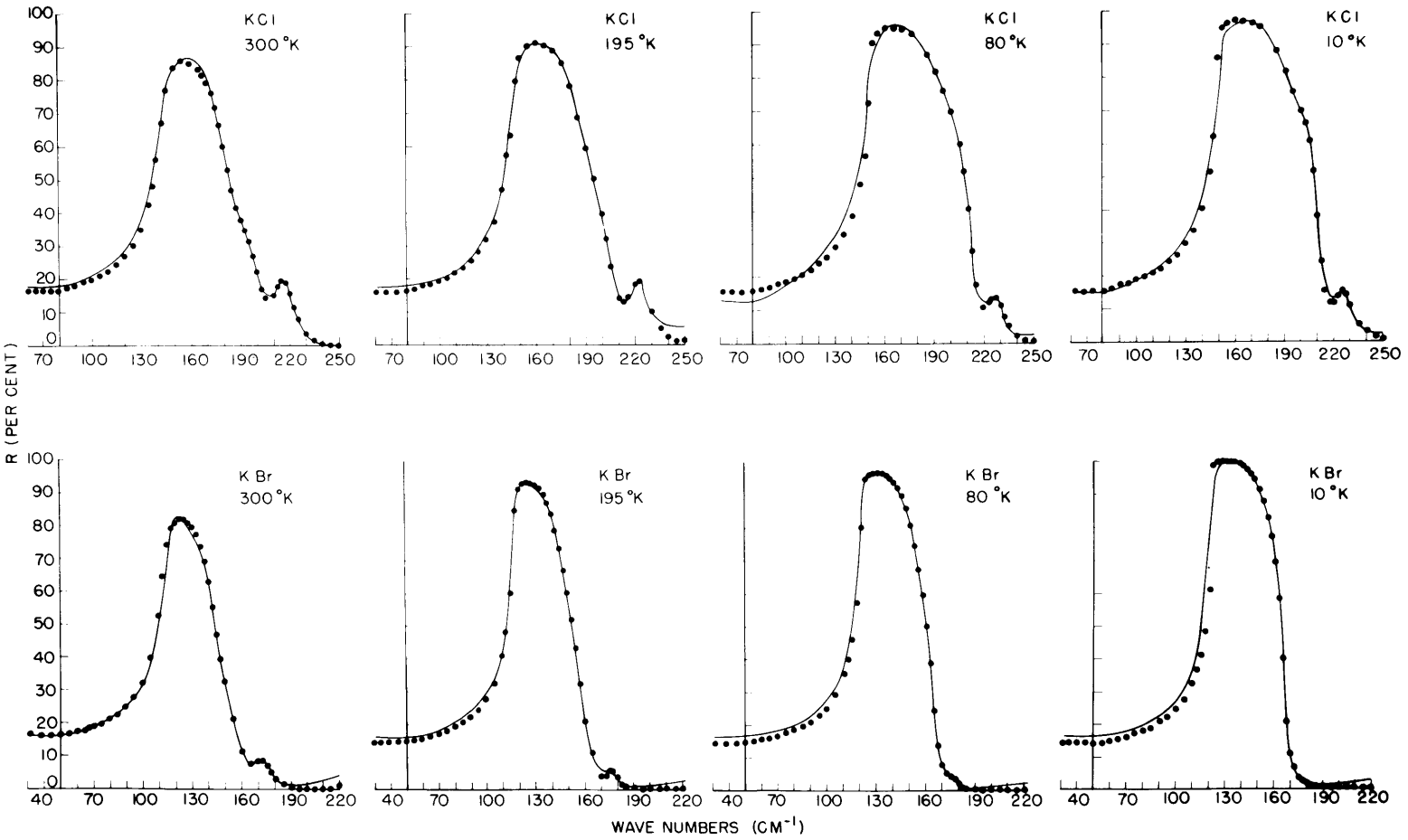

Fig. V-1. Reflectivity of KCl and KBr at various temperatures.
———— Measured.
. . . . . Calculated using classical dispersion analysis.

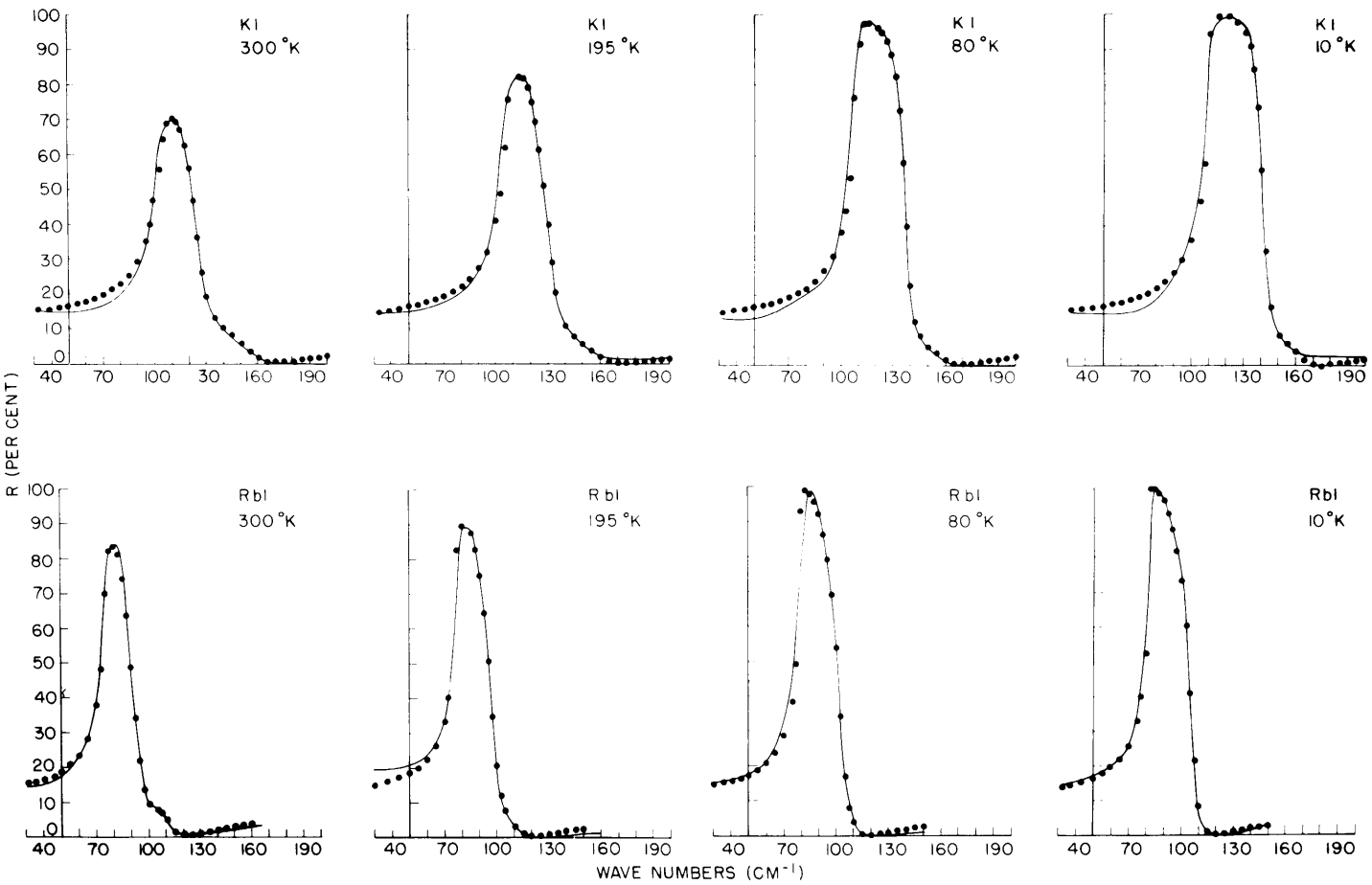

Fig. V-2. Reflectivity of KI and RbI at various temperatures.
———— Measured.
. . . . . Calculated.

Table V-1. Dispersion constants for alkali halides from classical oscillator fits.

		TO(Γ)					TO(x) + TA(x)			TO(x) + LA(x)							
		S_T	ω_T	$\omega_{TR}^{\dagger}$	γ_T	$\gamma_{TR}^{\dagger}$	S_1	ω_1	γ_1	S_2	ω_2	γ_2	ϵ_∞	ϵ_o	ω_L	ω_{LST}	e^*/e
KCl	(300°)	215	143	142	5	4.52	55	189.5	31	41	210.5	14.5	2.22	4.6	203	206	.77
KCl	(195)	223	147	146	3	3.36	48	190	32	48	216	18	2.22	4.63	210	213	
KCl	(80)	228	151	150	1.5	1.95	41	193	40	35	222.5	14	2.22	4.57	215	215	
KCl	(10)	238	150	151	1.0	1.36	37	193	30	36	221.5	14	2.22	4.59	214.5	214	
KBr	(300°)	172	113	114	5	4.67	42	150	28	36.5	169	15	2.43	4.9	158	161	.74
KBr	(195)	170	117	118	1.5	2.83	39	150	33	28	172	10	2.43	4.64	160	161	
KBr	(80)	174	120	122	0.8	1.59	31	156	28	18	174	12	2.43	4.58	164	164	
KBr	(10)	174	122	123	0.1	.86	24	157	28	19	176	23	2.43	4.5	165.5	166	
Kl	(300°)	147	103.5	102	6.6	6.22	50	136	28	48	148	36	2.82	5.08	135	138	.71
Kl	(195)	151	106	106	3.5	4.96	44	133	39	34	149	33	2.82	5.1	139	142	
Kl	(80)	157	108	108	0.5	2.7	24	137	28	44	151	25	2.82	5.05	143	144.5	
Kl	(10)	165	110	110	0.1	1.97				49	153	25	2.82	5.17	147	149	
Rbl	(300°)	103.5	75	75	2.2	2.8	31	92	21	35	105	16.5	2.71	4.84	99	100	.73
Rbl	(195)	107	77	77	1.3	2.08	31	93	30	28	106	21	2.71	4.82	100	103	
Rbl	(80)	108	80	80	0.1	1.45	31	94	30	18	108	17	2.71	4.67	103.5	105	
Rbl	(10)	109	82	82	0.03	1.14	27	94	23	12	106	11	2.71	4.57	105.5	106.5	

†From transmission measurements of Robert Lowndes.[2]

3. Data Analysis and Discussion

The reflectivity curves were fitted by machine programming using a dispersion analysis. By treating the interaction of E-M waves and the crystal lattice classically, the classical dispersion formula can be written for the complex dielectric constant as a function of frequency.[4]

$$\epsilon(\omega) = \epsilon_\infty + \sum_j \frac{S_j^2}{\omega_j^2 - \omega^2 + i\omega\gamma_j} = \epsilon' + i\epsilon'',$$

where the oscillator strength $S_j^2 = \epsilon_j'' \omega_j \gamma_j$; γ_j is the damping constant; ω_j is a transverse vibration frequency (ω_T has been designated the main transverse lattice frequency, and ω_L, the main longitudinal lattice frequency); ϵ_∞ is the dielectric constant at high frequencies and ϵ_o is the low-frequency dielectric constant. The dispersion constants used are given in Table V-1.

$$\omega_L(\mathrm{LST}) = (\epsilon_o/\epsilon_\infty)^{1/2},$$

ω_T is the calculated longitudinal frequency obtained by using the Lyddane-Sachs-Teller relation, and e^*, the effective charge on an ion, is obtained from the Szigetti relation

$$\omega_T^2 = \frac{4\pi N}{9m} e^{*2} \frac{(\epsilon_\infty+2)^2}{\epsilon_o - \epsilon_\infty},$$

where N is the number of ion pairs per unit volume, and m is the reduced mass of an ion pair. In Table V-1, comparison can also be seen between the ω_T and γ_T determined by Lowndes[2] and generally the agreement is within experimental error.

We have tentatively identified the frequency ω_1 with the multiphonon combination TO + TA, and ω_2 with TO + LA at the critical point 'X' in the Brillouin zone.

We are grateful to Professor A. Smakula and Mr. J. Kalnajs, of the Center for Materials Science and Engineering, M. I. T., for the samples.

Jeanne H. Fertel, C. H. Perry

References

1. G. O. Jones, D. H. Martin, P. A. Mauer, and C. H. Perry (to be published in Proc. Roy. Soc. (London)).
2. R. P. Lowndes, Ph. D. Thesis, University of London, 1967 (unpublished); R. P. Lowndes and D. H. Martin (to be published in Proc. Roy. Soc. (London)).
3. C. H. Perry, R. Geich, and E. F. Young, J. Appl. Opt. 5, 1171 (1966).
4. R. Geich and C. H. Perry, Quarterly Progress Report No. 77, Research Laboratory of Electronics, M. I. T., April 15, 1965, pp. 41-48.

B. INFRARED STUDIES OF KCl-KBr AND KI-RbI MIXED CRYSTALS

1. Introduction

A systematic study has been made of several solid solutions of the ion halides described in Section V-A in order to determine the lattice resonances and the variation of the observed vibrational frequencies with composition. New experimental results have been obtained for KCl_xBr_{1-x} and $K_xRb_{1-x}I$ which indicate that these studies may help develop a unified approach to the problem of suggesting criteria for predicting the behavior of the optical lattice modes of mixed crystals. The results presented in this report were obtained in exactly the same way as described previously; hence, the experimental procedure and data analysis will not be described here.

2. Discussion

Two types of mode behavior are normally observed for mixed crystals. In one class of mixed-crystal systems, the phonon frequency (of each of the modes, infrared or Raman active or both) varies continuously from the frequency characteristic of one end member to that of the other end member. The mode strength remains approximately constant, whereas the damping increases to a maximum in the region of the 50/50 material. This observation is often characterized as 'one mode' behavior and has been reported for several alkali halide crystals[1,2] $Ni_{1-x}Co_xO$,[3] and $(Ca, Ba)_{1-x}Sr_xF_2$[4,5] and is also typical of the result we find in the KCl-KBr system as shown in Figs. V-3, V-4, V-5, and V-6.

Reflection measurements were made on crystals grown from the melt and x-ray measurements, in most cases, indicated that the samples were all single phase. The only exception was the KCl 36.5% KBr 73.5% sample which showed that two slightly different compositions were present. Very little effect on the frequency is observed (see Figs. V-4 and V-5), but the damping constant for this sample is anomalously high (see Fig. V-6). The damping constant decreases slightly at low temperatures, but the same general shape is observed (see Fig. V-6). Table V-2 lists the dispersion constants KCl/KBr from the Kramers-Kronig analysis. Figure V-7 shows the variation of reflectivity with temperature for the 8% KBr:92% KCl sample. The main reststrahlen peak appears to consist of two peaks. From the values of the frequencies observed it would appear that the extra mode is too high for a localized Br^- mode in KCl which in any event would be situated in the optical-acoustic branches and be unobservable. It may, however, be a multiphonon process (TO+TA, for example) which is now showing up more predominantly on the high-frequency side of the reflectivity (the band at 210-225 cm^{-1} is probably TO+LA combination). Attempts were made to observe the same behavior in transmission in order to compare the frequency and damping constant with composition and temperature.[6] Unfortunately, although 'one mode' behavior was observed in

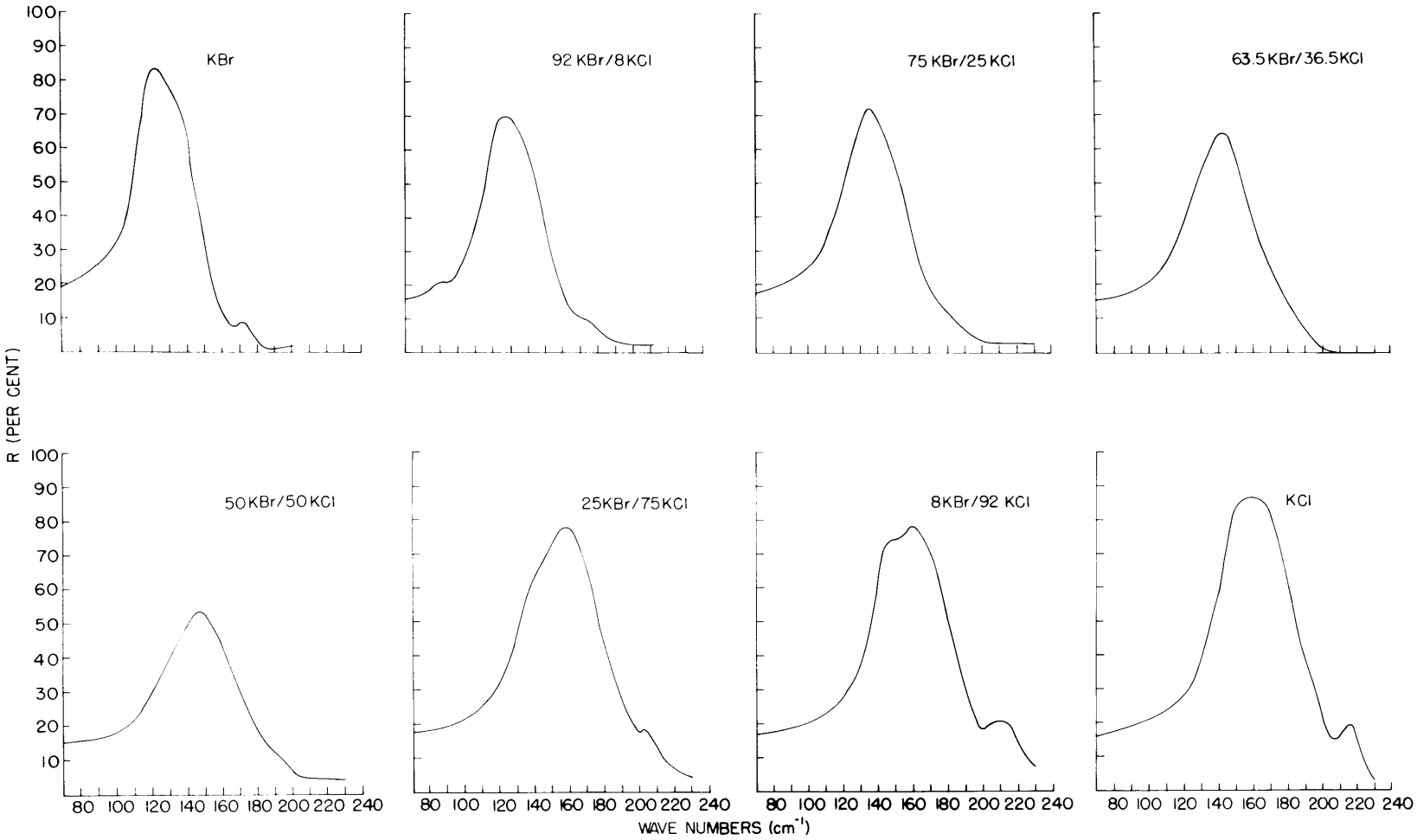

Fig. V-3. Reflectivity of KCl-KBr mixed crystals at 300°K.

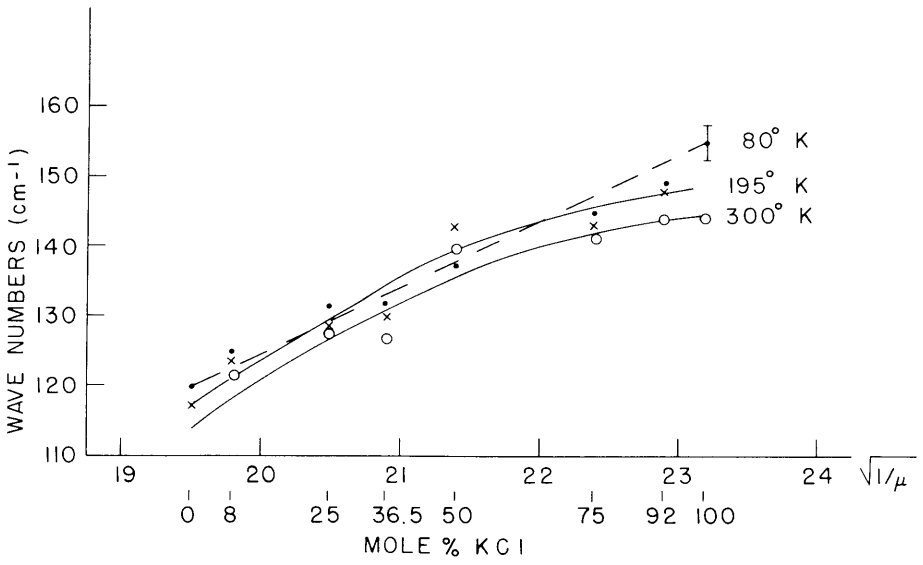

Fig. V-4. Variation of transverse optical frequency with composition for KCl-KBr.

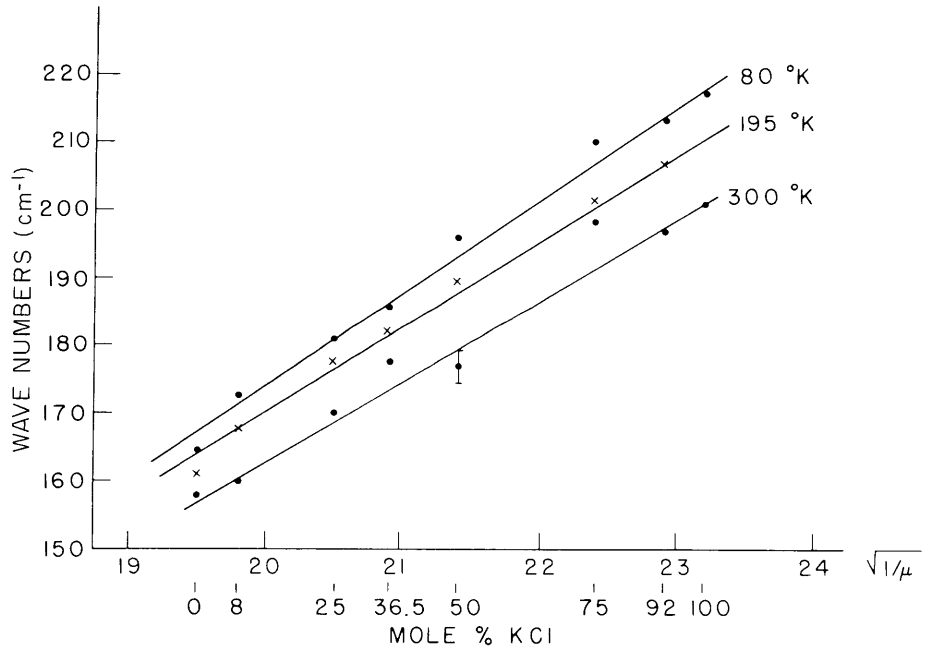

Fig. V-5. Variation of longitudinal optical frequency with composition for KCl-KBr.

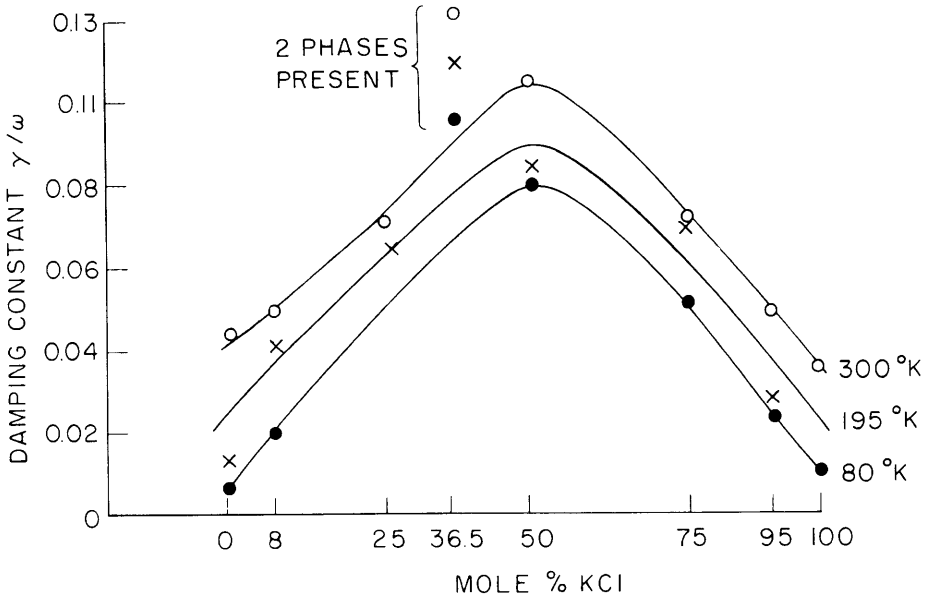

Fig. V-6. Variation of damping constant with composition and temperature. Note that the 36.5 mole % KCl sample has anomalously higher damping because of the effect of two phases.

transmission of thin evaporated films of the materials on polyethylene and crystal quartz substrates, the frequencies observed were all considerably higher in value than those obtained from the reflection measurements. It appeared that the composition of the thin films always favored the KCl end member and were not the same as the starting materials. As the necessary instrumentation to determine the compositions of the thin films was not available, these measurements were ignored.

In a second class of mixed crystals two phonon frequencies ('two mode' behavior) are observed to occur at frequencies close to those of the end members; the strength of each mode being approximately equal to the fractional formula weight of each component.

In the two-mode systems results have been reported only for covalent materials, for example, $GaAs_{1-x}P_x$,[7,8] $InAs_{1-x}P_x$,[9] $Ge_{1-x}Si_x$,[10] and those described in our earlier work on $CdS_{1-x}Se_x$.[11] For these covalent materials, the reststrahlen bands of the end members are well separated in frequency space.

In most of the 'one mode' systems there is frequency overlap between the reststrahlen bands (defined by the positions of the longitudinal and transverse frequencies) of the end components. Two-mode behavior has not been previously observed in any alkali halides. Examination of the list of crystals with gaps between the optical and acoustic branches and non overlap between the LO of the heavier member and the TO of the lighter member offers a very limited choice. As can be seen in Table V-1 the LO mode in RbI at room temperature occurs at ~99 cm^{-1} and the TO mode in KI is at

Table V-2. Dispersion constants for KBr/KCl from Kramers-Kronig analysis.

	ϵ_o	ϵ_∞	ω_{TO}	ω_{LO}	γ	S
KBr (300°K)	6.5	1.86	113.5	157.5	6	188
KBr (195°)	6.3	1.86	117.5	161	3	192
KBr (80°)	6.1	1.85	120	165	3	209
92KBr/8KCl (300°)	5.4	2.45	121.5	160	6	210
92KBr/8KCl (195°)	5.6	2.43	124	167.5	5	280
92KBr/8KCl (80°)	6.3	2.36	125	172.5	2.5	324
75KBr/25KCl (300°)	5.8	2.43	128	170	9	228
75KBr/25KCl (195°)	6.12	2.4	128.5	177.5	8.5	246
75KBr/25KCl (80°)	6.12	2.4	131.5	181	6.5	252
63.5KBr/36.5KCl (300°)	5.4	2.31	127	177.5	16.5	183
63.5KBr/36.5KCl (195°)	5.8	2.38	130	182	15.5	222
63.5KBr/36.5KCl (80°)	6.12	2.43	132	186	14	248
50KBr/50KCl (300°)	5.1	2.27	140	177	16	217
50KBr/50KCl (195°)	5.1	2.23	143	189.5	12	262
50KBr/50KCl (80°)	7.4	2.13	138	196	11	314
25KBr/75KCl (300°)	5.9	2.17	141.5	198.5	10	301
25KBr/75KCl (195°)	6.12	2.15	143	201.5	10	338
25KBr/75KCl (80°)	6.5	2.11	145	210	7.5	376
8KBr/92KCl (300°)	5.8	2.02	144	197	7	301
8KBr/92KCl (195°)	5.8	2.0	148	207	4	335
8KBr/92KCl (80°)	6.7	1.94	149	213.5	3.5	428
KCl (300°)	5.4	1.24	141	201	11	218
KCl (195°)	5.78	2.68	154	208	14.5	330
KCl (80°)	4.24	1.78	155	217.5	2.5	590 (?)

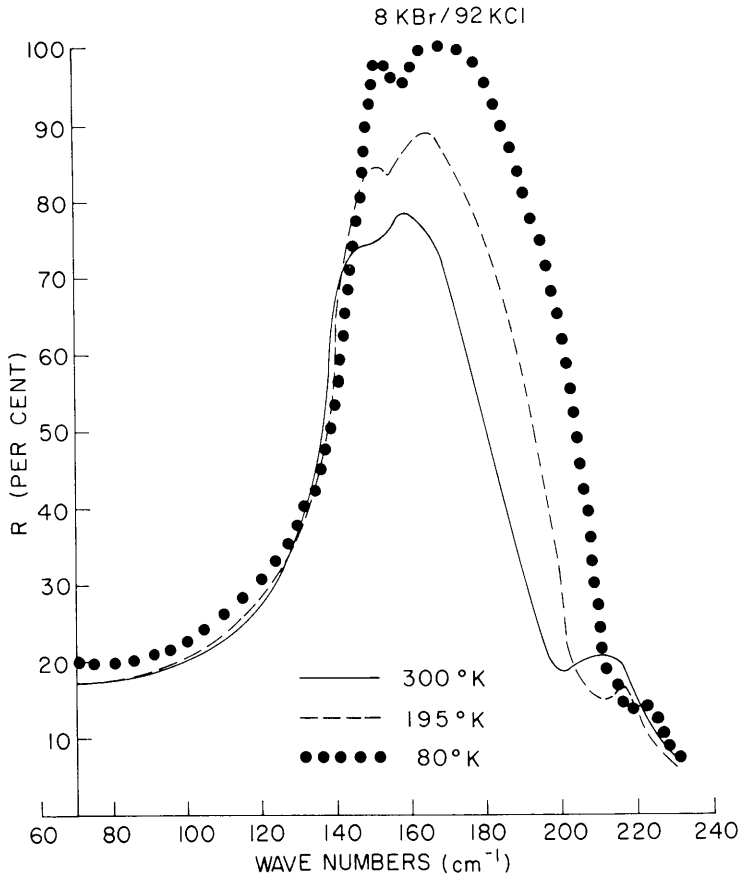

Fig. V-7. Variation of reflectivity with temperature for 8% KBr:92% KCl sample.

~106 cm^{-1}. KI is known to possess a gap between the optical and acoustical branches.[12] These two materials appeared to be an excellent choice for the investigation of possible two-mode behavior in an alkali halide mixed-crystal system.

Small mixed crystals of KI-RbI were obtained by dissolving the appropriate concentration in distilled water and slowly evaporating to dryness. The samples were carefully dried and pressed into pellets approximately 12 mm in diameter and 1-2 mm thick. Several samples were examined using x-ray techniques and the results indicated that KI-RbI forms solid solutions over the whole range of composition and that the lattice constant changes linearly with composition as seen in Fig. V-8.

Reflection measurements were taken at 300, 195, and 80°K and the results at 80°K were shown in Fig. V-9. Kramers-Kronig analysis of the reflectance data showed 'two mode' behavior over almost entirely the whole range of composition, as indicated in Fig. V-10, which is a plot of the imaginary part of the dielectric constant with frequency. The positions of the LO modes determined from peaks in the reciprocal of the

dielectric constant show essentially only 'one mode' behavior, although the 25% KI 75% RbI and the 5% KI 95% RbI give some indication of two modes appearing. This is displayed in Fig. V-11.

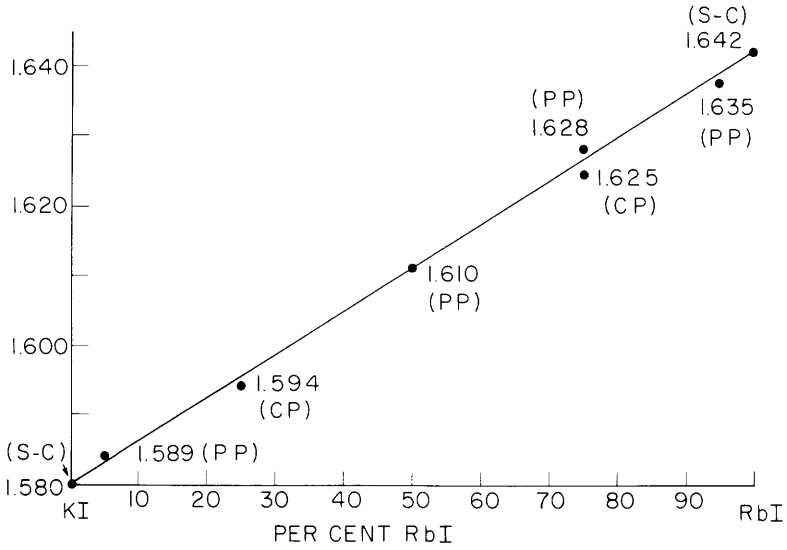

Fig. V-8. Lattice constant (in Ångstroms) of the KI-RbI mixed-crystal system at 300°K. (PP pressed pellet; CP crushed pellet; S-C single crystal.)

Thin-film transmission measurements of these materials were considerably more rewarding than the KCl-KBr system and 'two mode' behavior was also observed for the TO modes. The measurement of the LO frequency was obtained by using Berreman's technique [13] of oblique incidence transmission of a thin film evaporated onto a mirror using the infrared radiation polarized in the plane of incidence. Again the results were similar to the reflection measurements and only one mode was observed. The results of the transmission measurements to obtain the TO and LO modes are shown in Fig. V-12. The small sidebands on the low-frequency side of the LO mode are probably due to the angle of incidence, which causes some small interaction of the radiation with the TO modes. The band labeled "P" is due to polyethelene which was not completely removed in the ratioing process. Figure V-13 shows the variation of frequency with composition for measurements taken at room temperature. Good agreement can be seen between the Kramers-Kronig (K-K) data from the reflection measurements and the transmission data obtained from the thin lines. The gap mode labeled "G" of Rb^+ in KI was calculated from data provided by Genzel [14] and agrees well with the value obtained by extrapolating the TO_2 mode to 0% RbI. The dotted line represents the LO_2 mode calculated by using the modified Lyddane-Sachs-Teller relation

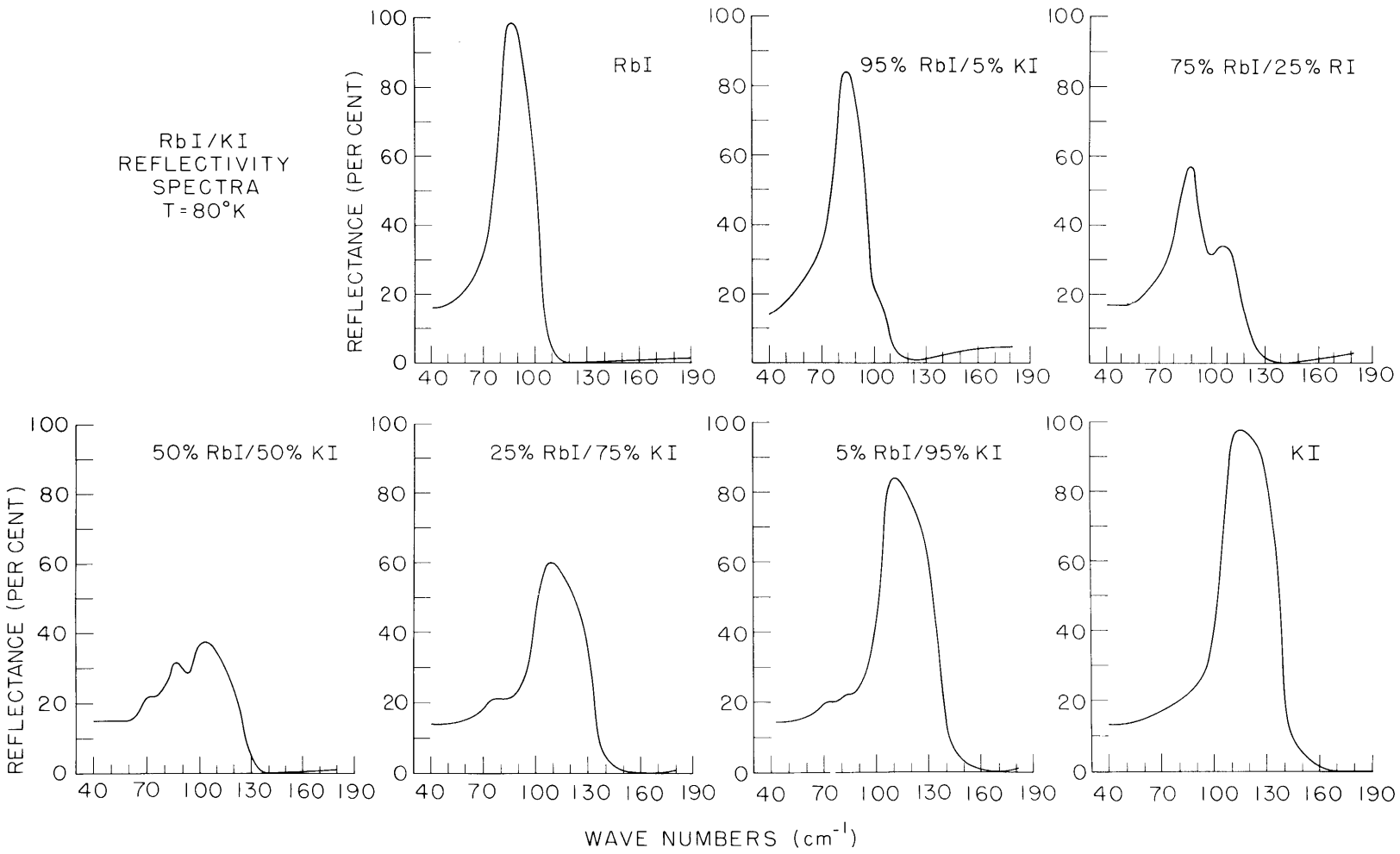

Fig. V-9. Reflectivity of KI-RbI mixed crystals at 80°K.

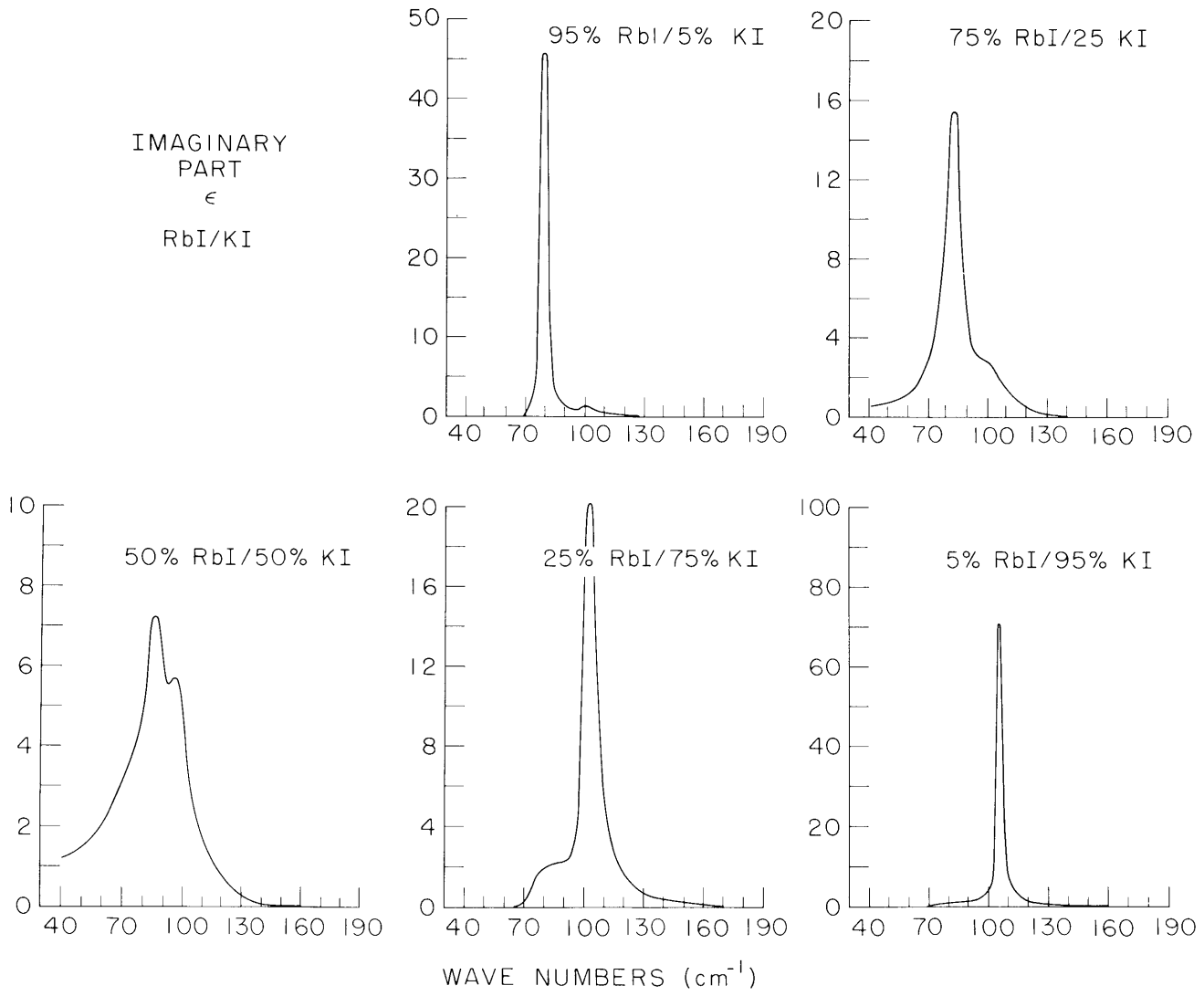

Fig. V-10. The imaginary part of the dielectric constant obtained from a Kramers-Kronig analysis of the data shown in Fig. V-9. Note the two transverse modes observed over almost the entire range of composition.

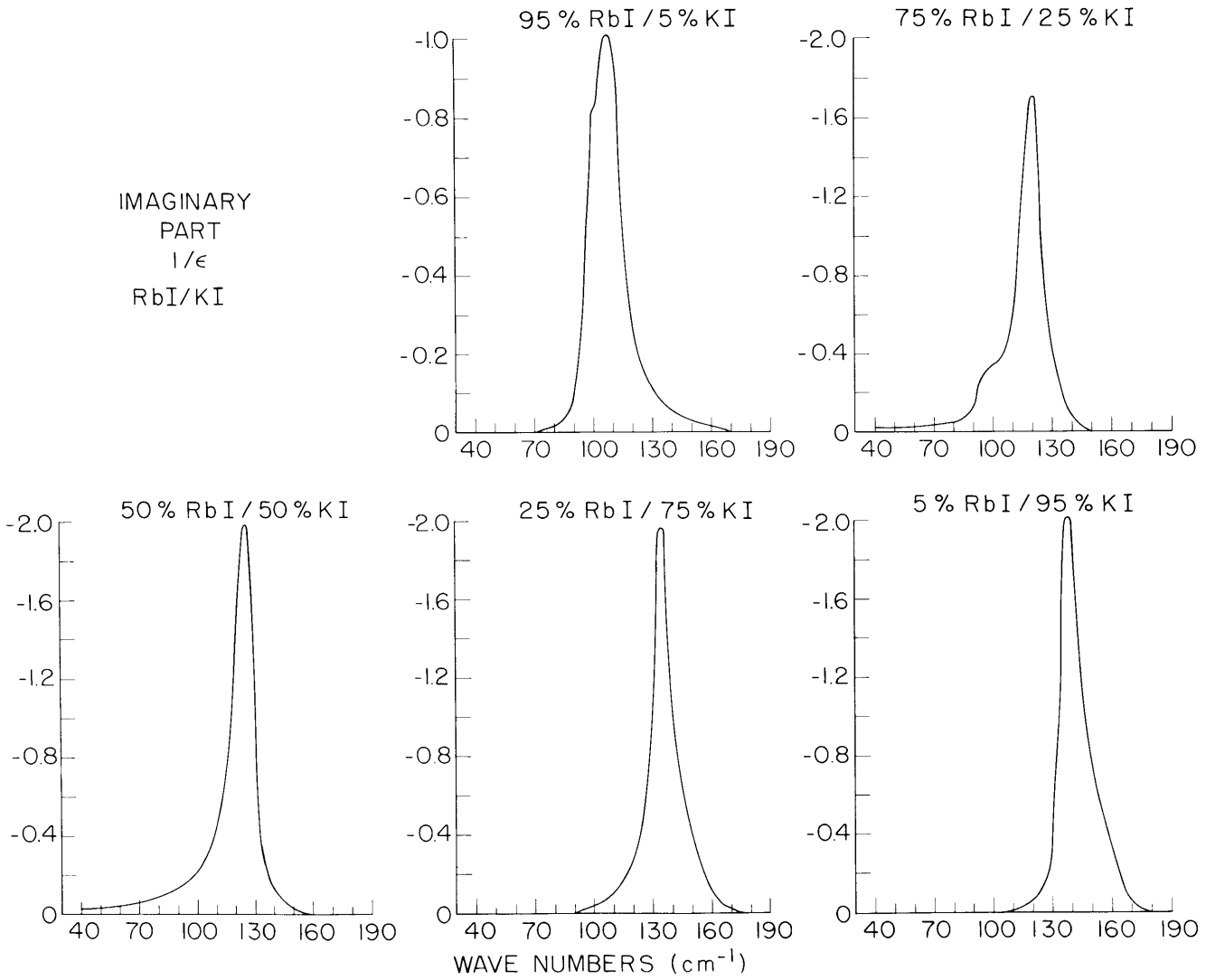

Fig. V-11. The reciprocal of the dielectric constant obtained from a Kramers-Kronig analysis of the data shown in Fig. V-9. Note that only one longitudinal mode is generally observed.

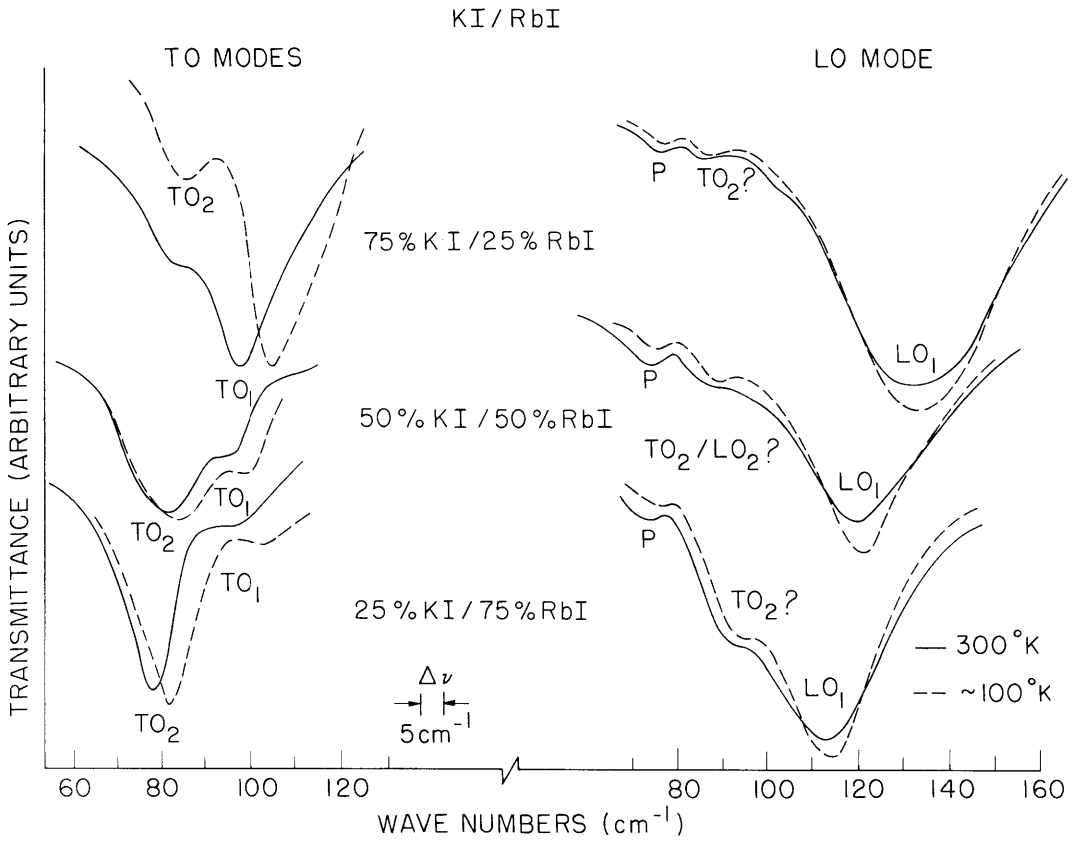

Fig. V-12. Thin-film transmission measurements to obtain the TO and LO for KI/RbI.

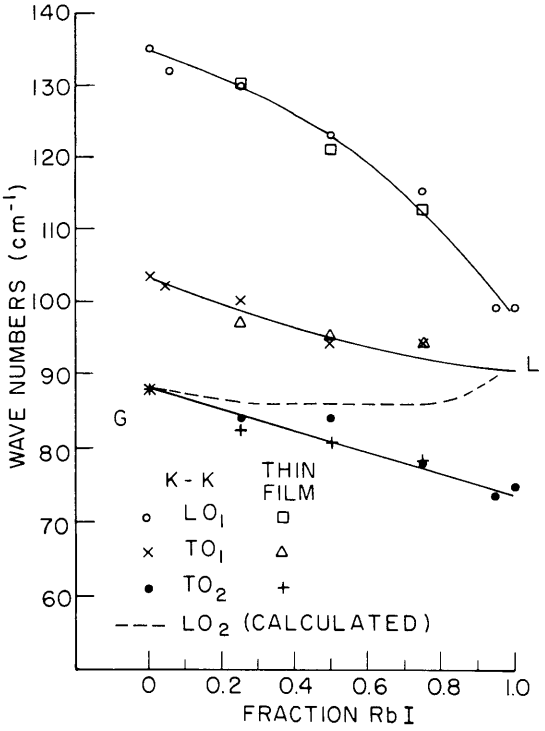

Fig. V-13. Variation of the TO and LO modes with composition at 300°K.

Table V-3. Frequencies for RbI/KI from Kramers-Kronig analysis.

	$\omega_{TO}^{(1)}$	$\omega_{TO}^{(2)}$	$\omega_{LO}^{(1)}$	$\omega_{LO}^{(2)}$-calc.
RbI (300°K)	75		99	
RbI (195°K)	77		100	
RbI (80°K)	80		103.5	
95RbI/5KI (300°K)	74		99	90
95RbI/5KI (195°K)	76		103 (98)	
95RbI/5KI (80°K)	79	101	107 (100)	
75RbI/5KI (300°K)	78	94	115	85.5
75RbI/5KI (300°K)	81	97	117	
75RbI/5KI (80°K)	83	98	120	
50RbI/50KI (300°K)	84	94	123	86
50RbI/50KI (195°K)	88	98	127	
50RbI/50KI (80°K)	85	96	125	
50RbI/50KI (10°K)	85	96	125	
25RbI/75KI (300°K)	84	100	131	86
25RbI/75KI (195°K)	83	102	133	
25RbI/75KI (80°K)	84	103	135	
5RbI/95KI (300°K)		102	132	89
5RbI/95KI (195°K)		105	136	
5RbI/95KI (80°K)		106	139	
5RbI/95KI (10°K)		106	141	
KI (300°K)	88[61]	103.5	135	
KI (195°K)		106	139	
KI (80°K)		108	143	

$$\frac{\epsilon_o}{\epsilon_\infty} = j \frac{\omega_{L_j}^2}{\omega_{T_j}^2}.$$

The point labeled "L" shows roughly where localized K^+ mode in RbI should be, but this falls completely inside the RbI optical branch and cannot be measured directly. The frequencies of RbI/KI obtained from the Kramers-Kronig analysis are given in Table V-3.

Various models have been used to describe the frequency variation in mixed-crystal systems. A linear chain model was used by Matossi[15] who calculated the vibrational frequencies of a one-dimensional ordered diatomic 50% mixed crystal xzyzxzyz. He considered only nearest-neighbor interactions, obtaining the force constants from the frequencies of the end member compounds, so that differences in the calculated frequency spectra derive solely from the mass differences in the isotopic substitution which generates the mixed crystal. When the mass of z is much heavier than the masses of x and y (such as for RbI/KI), two infrared frequencies are obtained which are very close to those of the end-member compounds. On the other hand, for KBr/KCl the model predicts one infrared active mode at a frequency approximately halfway between the frequencies of the end members and another (much weaker) one at a much lower frequency. The higher frequency mode predicted by this model for 50/50 crystals in the case of both KCl/KBr and RbI/KI agrees quite well with the experimental data. In the case of RbI/KI,

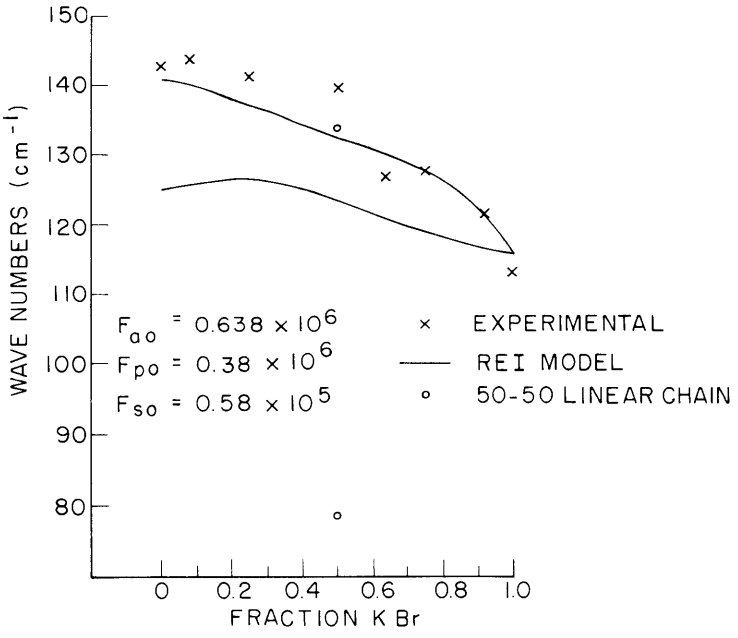

Fig. V-14. Experimental variation of the TO modes for the KCl/KBr system and the REI and linear chain model predictions.

however, the predicted value for the lower frequency mode is not at all near the observed frequency. For KCl/KBr, the weak lower frequency mode could not be observed at all,

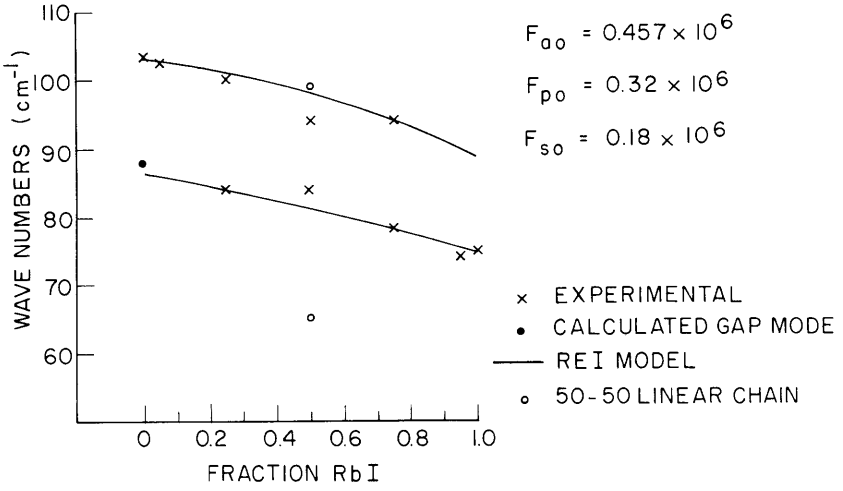

Fig. V-15. Experimental variation of the TO modes for the KI/RbI system and the REI and linear chain model predictions.

even in transmission measurements of samples 1 mm thick at 4°K. We have also been unable to observe the Raman active mode predicted by this model. This is no doubt due to the fact that our crystals are not ordered but random.

The Random Element Isodisplacement (REI) model[8] assumes that each of the atomic species vibrates with the same phase and amplitude. For the crystal AB_xC_{1-x}, the force constant between the A and B sublattices and that between the A and C sublattices are determined by the frequencies of the end-member compounds. The force constant F_{so} between the B and C sublattices is treated as an adjustable parameter which can be varied to give the best fit to the observed data. Thus next-nearest-neighbor interactions are also included. The results for KCl/KBr are shown in Fig. V-14 and for KI/RbI in Fig. V-15. In the case of RbI/KI the model can be made to fit the data quite satisfactorily and predicts the frequency dependence with composition for the two observed modes. The value obtained for F_{so} (the adjustable force constant between K-Rb) is of the same order of magnitude as those calculated for the K-I and Rb-I interactions, and is not as large as that needed to, say, fit $CdS_{1-x}Se_x$ which would be objectionably high. The fit of the model to the KCl/KBr data is less successful; in particular, a second mode occurring at lower frequency is predicted in addition to the main mode. This mode may be extremely weak, however, and may also not be observed because KCl does not have a gap between the optical and acoustic branches.

It would appear that the main problem with most of these models is that they are based on a one-dimensional lattice and consider only nearest and next-nearest-neighbor

interactions. For a complete description higher order interactions should be considered and a three-dimensional lattice should be used similar to that developed by Dawber and Elliot[16] and extended by Jaswal.[17] This has only been applied, however, to predicting localized and gap modes in Si,[18] GaAs,[19] NaI,[20] and CdS.[21]

We wish to thank Professor A. Smakula for the KCl-KBr samples and Mr. J. Kalnajs for the x-ray measurements and their interpretation.

Jeanne H. Fertel, C. H. Perry

References

1. F. Kruger, O. Reinkober, and E. Koch-Hohn, Ann. Physik 85, 110 (1928).
2. R. M. Fuller, C. M. Randall, and D. J. Montgomery, Bull. Am. Phys. Soc. 9, 644 (1964).
3. P. J. Gelisse, J. N. Plendl, L. D. Mansur, R. Marshall, and S. S. Mitra, J. Appl. Phys. 36, 2447 (1965).
4. R. K. Chang, B. Lacina, and O. S. Persham, Phys. Rev. Letters 17, 755 (1966).
5. H. W. Verleur and A. S. Barker, Jr., Bull. Am. Phys. Soc. 12, 81 (1966).
6. E. M. Immerman, S. B. Thesis, Department of Physics, M. I. T., 1967.
7. H. W. Verleur and A. S. Barker, Jr., Phys. Rev. 149, 715 (1966).
8. Y. S. Chen, W. Shockley, and G. L. Pearson, Phys. Rev. 151, A648 (1966).
9. F. Oswald, Z. Naturforsch. 14A, 374 (1959).
10. D. W. Feldman, M. Ashkin, and J. H. Parker, Jr., Phys. Rev. Letters 17, 1209 (1966).
11. J. F. Parrish, C. H. Perry, S. S. Mitra, O. Brafman, and I. F. Chang, Proc. Am. Phys. Soc. Meeting on II-VI Semiconducting Compounds, Providence, Rhode Island, September 1967, pp. 1100-1110.
12. I. G. Nolt, R. A. Westwig, R. W. Alexander, Jr., and A. J. Siemers, Phys. Rev. 157, 730 (1967).
13. D. W. Berreman, Phys. Rev. 130, 615 (1963).
14. L. Genzel, Private communication.
15. F. Matossi, J. Chem. Phys. 19, 161 (1951).
16. D. G. Dawber and R. J. Elliott, Proc. Roy. Soc. (London) A273, 222 (1963); Proc. Phys. Soc. (London) 81, 453 (1963).
17. S. S. Jaswal, Phys. Rev. 137, 302 (1965).
18. F. A. Johnson and W. Cochran, 1962 Proc. Int. Conf. on Physics of Semiconductors, Exeter, 1962, p. 498, London: Institute of Physics and Physical Society.
19. G. Dolling and J. L. T. Waugh, Proc. International Conference on Lattice Dynamics, J. Phys. Chem. of Solids 21 (Suppl.) 19 (1966).
20. A. M. Karo and J. R. Hardy, Phys. Rev. 129, 2024 (1963).
21. M. A. Nusimovici and J. L. Birman, Phys. Rev. 156, 925 (1967).

C. ERRATA: ON THE DIELECTRIC RESPONSE FUNCTION

In Quarterly Progress Report No. 90, July 15, 1968, the following errors have been noted.

Page 44.

Paragraph 1, line 7 should read:

The peak in ϵ''/ω occurs when $\partial(\epsilon''/\omega)/\partial\omega = 0$. Evaluating $\partial(\epsilon''/\omega)$ at $\omega = \omega_T$, we have

Paragraph 1, line 8 (left side of the equation) should read:

$$\left.\frac{\partial(\epsilon''/\omega)}{\partial\omega}\right|_{\omega=\omega_T} = \ldots$$

Paragraph 1, line 11 should read:

$$\therefore \left.\frac{\partial(\epsilon''/\omega)}{\partial\omega}\right|_{\omega=\omega_T} \leq 0 \ldots$$

Paragraph 1, line 12: change "peak of ϵ''" to read:

... peak of ϵ''/ω ...

Page 45.

Line after Eq. (17): change "minimum of η''" to read:

... minimum of η''/ω ...

J. F. Parrish